

# BACKCALCULATION OF AIRFIELD PAVEMENT STRUCTURES BASED ON WAVE PROPAGATION THEORY

By:

Kunihito Matsui<sup>1)</sup>, Yoshiaki Ozawa<sup>2)</sup> and Kazuya Takehara<sup>1)</sup>

1) College of Science and Engineering

Tokyo Denki University

Hatoyama Hiki Saitama 350-0394

Japan

Phone: +81(49) 296-2549; Fax: +81(49) 296-6501

[matsui@g.dendai.ac.jp](mailto:matsui@g.dendai.ac.jp)

2) Century-techno Inc.

Shin-Kotenbacho Bld. 7F

Nihonbashi Kodenba-cho Chuo-ku Tokyo 103-0001

Japan

PRESENTED FOR THE  
2010 FAA WORLDWIDE AIRPORT TECHNOLOGY TRANSFER CONFERENCE  
Atlantic City, New Jersey, USA

April 2010

## ABSTRACT

Nondestructive testing equipment called FWD (Falling Weight Deflectometer) has been widely utilized for structural evaluation of pavement. This paper presents backcalculation of multilayered pavement layer parameters from FWD tests by using dynamic backcalculation software which authors have recently developed. The theoretical solution for a system of axisymmetric wave propagation equations was developed using Hankel transform in radial direction and Fast Fourier Transform in time domain and was implemented into this backcalculation software. This software is called Wave\_BALM (Wave propagation based Back Analysis for Layer Moduli). The viscoelastic model used herein is called the Voigt solid (or Kelvin solid).

The validity of this software was examined by using FWD time history data of airfield pavement provided by FAA. Reliability of the results was confirmed by the following observations,

- 1) Backcalculation was conducted by using fifty sets of randomly generated seed values and the variation of the results was found small.
- 2) Excellent agreement between computed and measured deflections is confirmed.

## INTRODUCTION

The Falling Weight Deflectometer (FWD) is the most commonly used equipment for nondestructive evaluation of pavement systems. Although the FWD test is dynamic, the backcalculation techniques used to the FWD records are primarily elastostatic based approach. Only peaks of load and response histories are used in the backcalculation and valuable information which may contain in the time series data is disregarded. The discrepancy may lead to systematic errors in the estimation of pavement moduli.

When an impulsive force applies at pavement surface, deformation wave propagates in all directions from the center of loading. FWD measures the propagating deformation wave at several points of pavement surface. In general, it is well known that damping effect must be taken into consideration. The number of investigations have focused on the dynamic interpretation of FWD data have been reported [1-5]. Many of them utilize the finite element code for the dynamic analysis of pavement structures.

Thus, authors have derived the analytical solution for a wave propagation problem in a viscoelastic multilayered media[6]. The solution code called WPALS (Wave Propagation Analysis for Layered Systems) was developed and implemented in the backcalculation software called Wave\_BALM (Wave propagation based Back Analysis for Layer Moduli) [7]. It is assumed that all layers are composed of viscoelastic solid represented by the Voigt model.

The FWD time history data utilized in this study were measured at the Federal Aviation Administration's National Airport Test Facility. Layer moduli and damping coefficients of airfield pavement estimated by Wave\_BALM are herein reported.

## WAVE PROPAGATION ANALYSIS IN VISCOELASTIC MEDIA

Impulse load acts uniformly on a circular area of radius  $r_0$  at the surface of multilayered half space composed of the Voigt model. This is an axisymmetric problem and the following wave equations holds in all layers (see Figure 1),

$$\frac{\partial \sigma_r}{\partial r} + \frac{\partial \tau_{rz}}{\partial z} + \frac{\sigma_r - \sigma_\theta}{r} = \rho \frac{\partial^2 u}{\partial t^2} + c \frac{\partial u}{\partial t} \quad (1a)$$

$$\frac{\partial \tau_{rz}}{\partial r} + \frac{\partial \sigma_z}{\partial z} + \frac{\tau_{rz}}{r} = \rho \frac{\partial^2 w}{\partial t^2} + c \frac{\partial w}{\partial t} \quad (1b)$$

in which  $u$  and  $w$  are displacement components in  $r$  and  $z$  directions,  $\rho$  is density,  $c$  is density proportional damping, and  $\sigma_r, \sigma_\theta, \sigma_z$  and  $\tau_{rz}$  are normal and shearing stresses respectively.  $\tau_{\theta r}$  and  $\tau_{\theta z}$  are disregarded because of axisymmetry assumption and thus they are not shown in Figure 1.

The following set of equations gives strain- displacement relationship.

$$\varepsilon_r = \frac{\partial u}{\partial r}, \varepsilon_\theta = \frac{u}{r}, \varepsilon_z = \frac{\partial w}{\partial z}, \gamma_{rz} = \frac{\partial u}{\partial z} + \frac{\partial w}{\partial r} \quad (2)$$

in which  $\varepsilon_r, \varepsilon_\theta$  and  $\varepsilon_z$  are normal strains corresponding to  $\sigma_r, \sigma_\theta$  and  $\sigma_z$ , and  $\gamma_{rz}$  is shearing strain corresponding to  $\tau_{rz}$ .

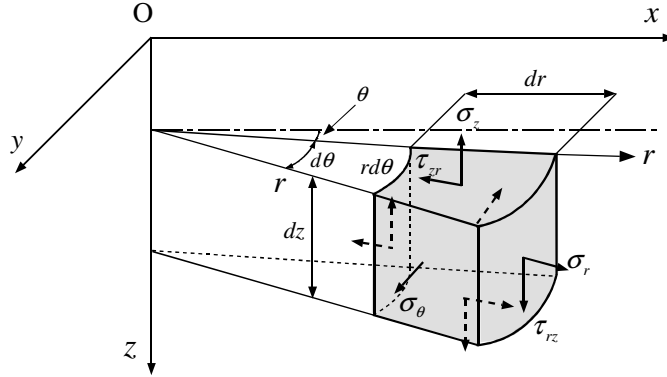


Figure 1 definition of stresses in the axisymmetric coordinate

The stress-strain relationship for the Voigt model can be expressed as,

$$\begin{Bmatrix} \sigma_r \\ \sigma_\theta \\ \sigma_z \\ \tau_{rz} \end{Bmatrix} = \left( E + F \frac{d}{dt} \right) \begin{pmatrix} a+2b & a & a & 0 \\ a & a+2b & a & 0 \\ a & a & a+2b & 0 \\ 0 & 0 & 0 & b \end{pmatrix} \begin{Bmatrix} \varepsilon_r \\ \varepsilon_\theta \\ \varepsilon_z \\ \gamma_{rz} \end{Bmatrix} \quad (3)$$

where ,

$$a = \frac{\nu}{(1+\nu)(1-2\nu)} , b = \frac{1}{2(1+\nu)}$$

$E$  is Young's modulus,  $F$  is damping coefficient ( also called as viscous coefficient) and  $\nu$  is Poisson's ratio . These material properties may differ but the relationships of Equations (1)-(3) hold in all layers.

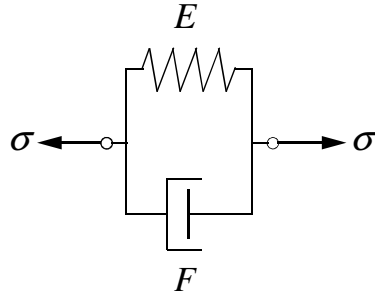


Figure 2 Voigt Model [8]

If the finite element method (FEM) was applied to solve Equations (1)-(3), it would result in a system of equations of motion with a Rayleigh damping matrix which is expressed by a linear combination of mass and stiffness matrices. In this formulation the parameter  $c$  appears in the mass matrix proportional damping and  $F$  comes in the stiffness matrix proportional damping.

When impulsive force  $P(t)$  acts uniformly over a circular area of radius  $r_0$  at the surface of multilayered system, the boundary condition can be written as,

$$\sigma_z(r,0,t) = -p(t) \quad |r| \leq r_0 \quad (4a)$$

$$= 0 \quad |r| > r_0 \quad (4b)$$

$$\tau_{rz}(r,0,t) = 0 \quad r \geq 0 \quad (4c)$$

where

$$p(t) = P(t)/(\pi a^2)$$

Instead of using FEM, we have derived the analytical solution of Equations (1)-(4) using Hankel transform and Fast Fourier Transform (FFT) [6].

## BACKCALCULATION

The parameters  $E, F$  and  $c$  are unknown and need to be identified. However our past work found  $c$  insignificant [7]. Thus,  $E$  and  $F$  of pavement layers are identified from FWD time history data. Let  $E_j$  and  $F_j$  are unknown parameters of the  $j$ th layer ( $j = 1, \dots, M$ ). And  $w_i(t)$  be the measured deflection at sensor location  $i$  ( $i = 1, \dots, N$ ) and  $z_i(E_j, F_j, t)$  be a computed deflection at the corresponding location.  $E_j$  and  $F_j$  are determined such that  $z_i(E_j, F_j, t)$  shows a good agreement with  $w_i(t)$  at discrete time step by using a point matching technique. The comparison is made in the range where responses are large, because the heads and tails of measured responses are likely to contain significant errors. The total number of unknown parameters are  $2M$ , when the number of pavement layers are  $M$ .

The seed values  $\mathbf{X} = (E_j, F_j)^T$  of all layers are assigned prior to backcalculation. Then surface deflections are computed and the difference between computed and measured deflections in the selected range is minimized by the Gauss-Newton method with truncated singular value decomposition to determine the unknowns. The evaluation function is defines as follows.

$$J = \frac{1}{2} \sum_{l=1}^L \sum_{i=1}^N \sum_{k=1}^K \{w_i^{(l)}(t_k) - z_i^{(l)}(\mathbf{X}, t_k)\}^2 \quad (5)$$

in which ,

$w_i^{(l)}(t_k)$  : measured response of the point  $i$  at time  $t_k$  in  $l$ -th data set.

$z_i(\mathbf{X}, t_k)$  : computed response of the point  $i$  at time  $t_k$ .

$\mathbf{X}$  : the vector of unknown parameters (layer moduli and damping coefficients)

$K$  : the number of discrete time steps.

$L$  : the number of data sets used for backcalculation.

Since this is a nonlinear minimization problem, iterative computation must be introduced. The following is the update formula to estimate unknown parameters [8].

$$\begin{aligned} & \sum_{\ell=1}^L \sum_{m=1}^{2M} \sum_{k=1}^K \left\{ \sum_{i=1}^N \frac{\partial z_i^{(\ell)}(\mathbf{X}, t_k)}{\partial X_n} \frac{\partial z_i^{(\ell)}(\mathbf{X}, t_k)}{\partial X_m} \right\} dX_m \\ &= \sum_{\ell=1}^L \sum_{k=1}^K \sum_{i=1}^N (u_i^{(\ell)}(t_k) - z_i^{(\ell)}(\mathbf{X}, t_k)) \frac{\partial z_i^{(\ell)}(\mathbf{X}, t_k)}{\partial X_n} \end{aligned} \quad (6)$$

$n = 1, \dots, 2M$

Equation(6) becomes simultaneous equations of  $2M \times 2M$ . Since the condition number of coefficient matrix often becomes large, the set of equations must be solved with care. A method such as a truncated singular matrix decomposition method will help to solve the problem.

Measured and computed deflections are compared at every time step in the time interval  $t_1 \leq t \leq t_K$  and the square sum of the difference is minimized. The time when the deflection of loading plate center D0 exceeds 50% of its peak deflection is defined as  $t_1$  and the time when the deflection of 150cm off from the center reduces less than 50% of its peak is defined as  $t_K$  as shown in Figure 3. The time increment of 0.2652 ms is used from the FWD data.

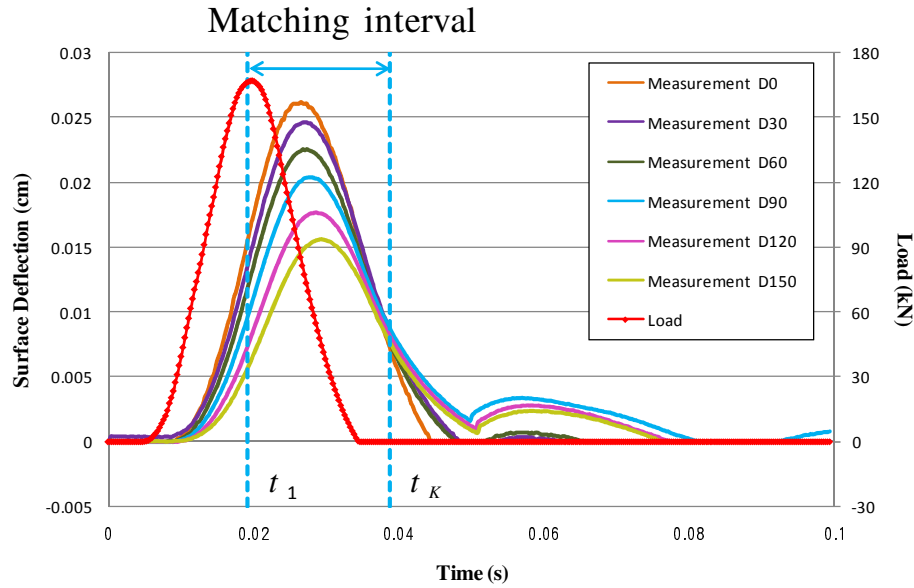


Figure 3 The interval of point-wise matching

## DESCRIPTION OF CROSS SECTIONS AND MATERIALS

The U.S. Federal Aviation Administration's National Airport Pavement Facility (NAPTF) is a full scale pavement test facility. The NAPTF was constructed to generate full-scale testing data to investigate the airport pavement performance. FWD tests were conducted on the NAPTF pavement test sections. The description of cross sections FWD tests were conducted is given in Table 1.

All tests were carried out by four drops with the target loads 36,000, 12,000, 24,000 and 36,000 lbs (1 lb = 4.4482N). The first three drops recorded the peak values of loads and deflections and the fourth drop the time histories of loads and deflections. Only the time history

data from the fourth drop is employed to estimate layer parameters in this paper. However, the cross section (Point ID: LRS/LFS Trans Area Slab 1 C01) was not analyzed because it is not axisymmetry due to the thickness variation of layer 2. The forward analysis implemented in Wave\_BALM requires uniform layer thickness. Although all units of the original data are in US units, they were converted to SI units because the backcalculation software can accept only SI units.

Table 1 Information of pavement structures for all points

Point I.D	Layer 1	Layer 2	Layer 3	Layer 4	Files
LRS C01 (Section1)	20' by 20' PCC Slab H = 11 inch	P306 Econo=crete H = 6.125 inch	P154 material H = 8.375 inch	Low Strength Sub-grade	GRAPHA & GRAPHB
LRS/LFS Trans Area Slab 1 C01	12.5' by 20' PCC slab H=17.125 in	P209, H varied from 8.375 to 23.5 inch	Low Strength Sub-grade		GRAPHC & GRAPHD
LFS A09 @ C/L (Section2)	P401 asphalt, H = 5 inch	P401, Asphalt stabilized base, H=4.875 inch	P154 sub- base, 29.625 inch	Low Strength Sub-grade	GRAPHE & GRAPHF, (No loading area)
LFS F11, Lane 2 (Section2)	P401 Asphalt, H = 5 inch	P401, Asphalt stabilized base, H=4.875 inch	P154 sub- base, 29.625 inch	Low Strength Sub-grade	GRAPHG & GRAPHH (Loading area)
LFC F13, Lane 2 (section 3)	P401 Asphalt, H = 5 inch	P209, Crushed Stone, H = 7.75 inch	P154 sub- base, H = 36.375 in	Low Strength Sub-grade	GRAPHI & GRAPHJ (Loading area)
LFC A09 @ C/L (Section 3)	P401 Asphalt, H = 5 inch	P209, Crushed Stone, H = 7.75 inch	P154 sub- base, H = 36.375 in	Low Strength Sub-grade	GRAPHK & GRAPHL (No loading area)
HFC @ C/L (Section 4)	P401 Asphalt, H = 5.25 inch	P209, Crushed Stone, H = 10.875 inch	High strength Sub- grade		GRAPHM & GRAPHN (No loading area)
HFC Lane 2 (Section4)	P401 Asphalt, H = 5.25 inch	P209, Crushed Stone, H = 10.875 inch	High strength Sub- grade		GRAPHO & GRAPHP (Loading area)

1 inch = 2.54 cm

'Loading area' in sections 2, 3 and 4 means that 20,000 to 30,000 loading passes (B777 and B747 gear) have been applied and 'no loading area' refers to the center of pavement where no heavy load has been applied.

## CROSS SECTIONS AND BACKCALCULATION RESULTS

LFS A09@C/L and LFS 11, Lane 2, LFC F13, Lane 2 and LFC A09@C/L, and also HFC@C/L and HFC Lanes 2 in Table 1 have same cross sections and same materials. Thus there are four cross sections which are given in Table 2 in SI units. Since the section 2 contains asphalt stabilized layer, backcalculation was conducted on 4 layer and 3 layer systems (section2-1 and section 2-2 respectively).

Table 2 Cross Sections Used for Backcalculation

### Section 1 (LRS)

	material	density(kg/m <sup>3</sup> )	Poisson's ratio	thickness(m)	range of seed modulus (MPa)
layer 1	PCC Slab	2450	0.2	0.279	20,000 - 50,000
layer 2	Econo crete	2400	0.2	0.156	15,000 - 30,000
layer 3	Sub-base	2242	0.35	0.213	100 - 600
layer 4	Sub-grade	1949	0.4		20 - 100

### Section 2-1 (LFS)

	material	density(kg/m <sup>3</sup> )	Poisson's ratio	thickness(m)	range of seed modulus (MPa)
layer 1	Asphalt	2300	0.35	0.127	5,000 - 10,000
layer 2	As stabilized	2300	0.35	0.124	5,000 - 10,000
layer 3	Sub-base	2242	0.35	0.752	500 - 1,000
layer 4	Sub-grade	1949	0.4		20 - 100

### Section 2-2 (LFS)

	material	density(kg/m <sup>3</sup> )	Poisson's ratio	thickness(m)	range of seed modulus (MPa)
layer 1	As compsite	2300	0.35	0.251	5,000 - 10,000
layer 2	Sub-base	2242	0.35	0.752	500 - 1,000
layer 3	Sub-grade	1949	0.4		20 - 100

### Section 3 (LFC)

	material	density(kg/m <sup>3</sup> )	Poisson's ratio	thickness(m)	range of seed modulus (MPa)
layer 1	Asphalt	2300	0.35	0.127	5,000 - 10,000
layer 2	Crushed Stn	2545	0.35	0.197	1,000 - 3,000
layer 3	Sub-base	2242	0.35	0.924	500 - 1,000
layer 4	Subgrade	1949	0.4		20 - 100

### Section 4 (HFC)

	material	density(kg/m <sup>3</sup> )	Poisson's ratio	thickness(m)	range of seed modulus (MPa)
layer 1	Asphalt	2300	0.35	0.133	5,000 - 10,000
layer 2	Crushed Stn	2545	0.35	0.276	1,000 - 3,000
layer 3	Subgrade	2095	0.4		100 - 500

There are two sets of time history data for Section 1. From section 2 to section 4, there are two sets each of time history data at both no loading area and loading area. Backcalculation was performed using each set of data and also two sets of data combined. When each set of data is used,  $L$  in Equation (5) is 1, while  $L$  is 2 when two sets are used. Because backcalculation tends to be unstable, fifty sets of seed values are randomly generated for backcalculation in the ranges described in Table 2. Layer modulus and layer damping are computed and their mean and standard of deviation are presented in Tables 3 and 4

Section 1 is PCC Slab section. The backcalculated modulus of layer 1 shows about 24,000 MPa, the modulus of layer 2, which is econocrete, is about 13,000 MPa. In this backcalculation, curling effects are not considered and full interface bonding is assumed.

For Section 2, FWD tests were conducted at no loading area and loading area. Although Section 2 is a four layer system, backcalculation is made on both a four layer system and three layer in which layer 1 and layer 2 are combined and considered as one asphalt composite layer. The results from the four layer system show the backcalculated modulus of layer 1 is about 8400 MPa, and that of layer 2 is about 5,000 MPa in no loading area. The backcalculated modulus of combined layer is about 6800 MPa, which is about the average of layers 1 and 2 of the four layer system. Layer moduli of sub-base and subgrade estimated from the four and three layer systems remain unchanged. The table shows that estimated moduli in loading area are smaller than those in no loading area. The marked reduction of layer moduli is observed in upper layers than in lower layers.

For Section 3, the moduli of layers 1 and 2 are about 7800 MPa and 350 MPa respectively in no loading area while those moduli in loading area show noticeable reduction and their values are about 4000 MPa and 200 MPa respectively. Significant stiffness reduction takes place mainly in upper layers. Little difference is observed in the subgrade moduli of no loading area and loading area.

For Section 4, the backcalculated layer modulus of layer 1 is about 11,000 MPa, that of layer 2 is about 100 MPa, and that of layer 3 is about 370 MPa. As described in Table 1, the subgrade is high strength subgrade. The backcalculated modulus is much higher than those of other sections. On contrary to our expectation, clear reduction is not observed in upper layer moduli of loading area. Although the subgrade modulus of loading area shows slight reduction, the upper layer moduli shows a little increase in loading area. These unexpected results may occur due to densification of upper layers when the subgrade is very stiff.

Table 4 presents the backcalculated layer dampings. It is not known what results imply up to now. It can be said that the larger the layer modulus is, the larger its damping coefficient is when layer material is same. Also it can be said that the value of layer damping is in general one percent or less of that of layer modulus.

Table 3. Backcalculated Layer Modulus (MPa)

	Pavement Surface Temperature(°C)		Layer 1			Layer 2			Layer 3			Layer 4		
			Set 1	Set 2	Combined	Set 1	Set 2	Combined	Set 1	Set 2	Combined	Set 1	Set 2	Combined
Section 1 (LRS)	16	-	24714	24755	24471	12316	12648	12751	144	145	149	95	94	93
			1473	1446	1610	1393	1255	1381	30.7	31.7	32.4	2.7	2.5	2.5
Section 2-1 (LFS)	16	No loading area	8229	8676	8411	4944	5247	5053	136	130	134	107	109	107
			1845	1736	1803	974	853	923	9.2	12.0	8.6	4.2	4.9	4.0
Section 2-2 (LFS)	16	No loading area	6640	7124	6777	-	-	-	124	121	123	111	106	111
			132	31	162	-	-	-	8.1	1.5	10.0	3.6	2.0	4.1
Section 2-1 (LFS)	15	Loading area	7826	6696	7742	3720	4075	3751	114	127	115	101	100	101
			2119	1969	1940	808	900	793	9.6	13.7	9.7	3.9	4.9	4.2
Section 2-2 (LFS)	15	Loading area	5865	5692	5816	-	-	-	102	113	102	100	104	106
			25	169	138	-	-	-	1.2	10.9	8.7	1.4	4.2	3.9
Section 3 (LFC)	15	No loading area	7560	8166	7799	349	349	350	104	104	104	120	120	120
			379	377	378	39	39	39	3.9	3.9	3.9	2.5	2.4	2.5
Section 3 (LFC)	16	Loading area	3622	4444	3936	197	216	205	72	75	73	114	115	114
			111	133	111	14	16	13	1.7	1.7	1.6	0.9	1.0	1.2
Section 4 (HFC)	15	No loading area	10724	11630	11071	103	105	104	368	372	369	-	-	-
			4.9	4.9	5.1	0.2	0.3	0.2	0.2	0.1	0.2	-	-	-
Section 4 (HFC)	16	Loading area	11489	11382	11456	129	141	134	312	308	310	-	-	-
			8.2	13.8	9.5	0.3	0.4	0.4	0.2	0.2	0.2	-	-	-

Table 4. Backcalculated Layer Damping (MPa.s)

[illegible]

The backcalculated results depend on the assumed layer density, Poisson's ratio, layer thickness and ranges of seed values, although their effects on the results differ.

When FFT is applied to  $E + F d/dt$  in Equation (3), it becomes complex modulus of  $E^* = E + i(2\pi f)F$ , in which  $i = \sqrt{-1}$  and  $f$  is frequency (Hz). Thus its magnitude can be expressed as,

$$|E^*| = \sqrt{E^2 + (2\pi f F)^2} \quad (7)$$

When a stationary load is applied,  $f$  is 0,  $|E^*| = E$  from the above equation.  $|E^*|$  increases with the increase of  $f$ . Figure 4 illustrates the magnitude of layer complex modulus in section 3 (loading area). The figure explains that a layer modulus appears stiff when a loading duration is short. When stationary load is applied, the modulus decreases to the modulus values of Table 3.

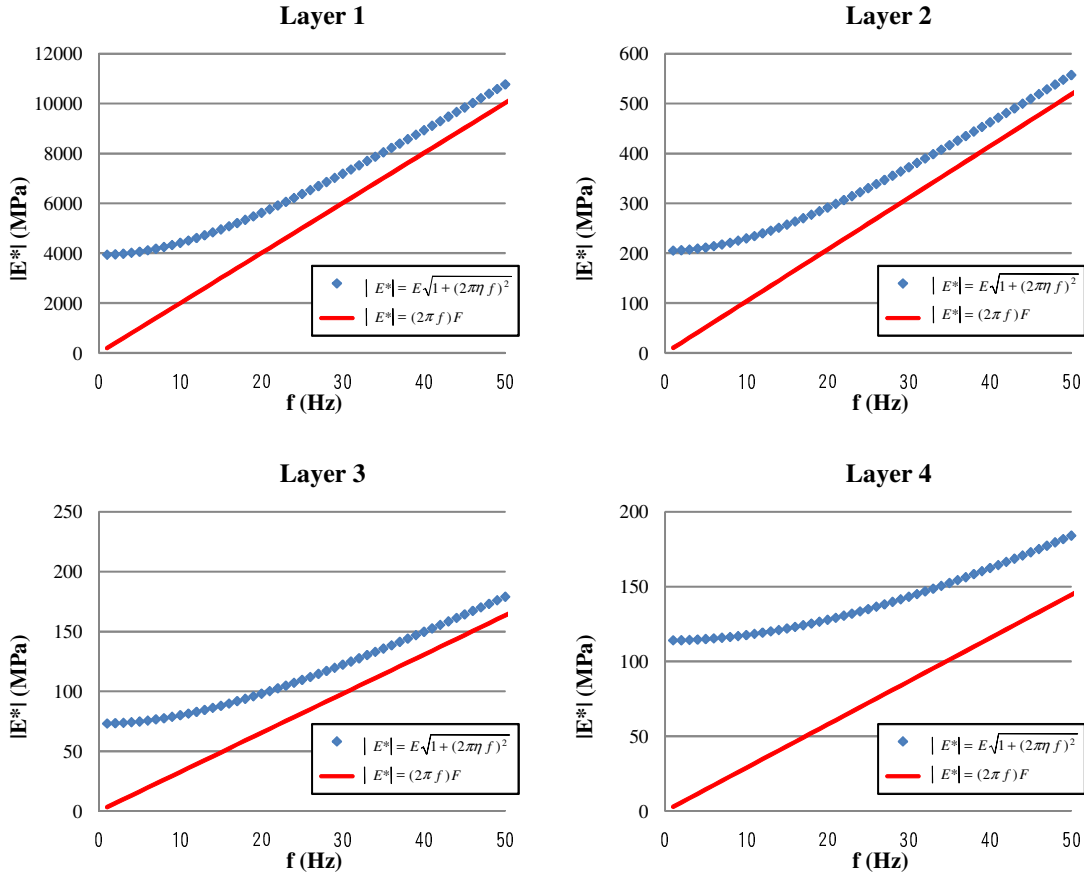


Figure 4 Relationship between the magnitude of complex layer modulus and frequency

## COMPARISON OF MEASURED AND COMPUTED DEFLECTIONS

Measured deflections are compared with computed deflections after backcalculation in Figures 4(a) – 4(d). Figure 4(a) illustrates the deflections from No.1 of Section 1. Figure 4(b) describes the deflections from No.1 of Section 2 in loading area. Figure 4(c) shows the deflections from No.1 of Section 3 and Figure 4(d) shows those of Section 4 in loading area.

The deflections are matched by upgrading parameter values using Equation (6) in the pre-assigned time interval. All figures demonstrate excellent agreement between measured and computed deflections. Judging from the good agreement, it can be stated that the backcalculation results presented herein are quite reliable.

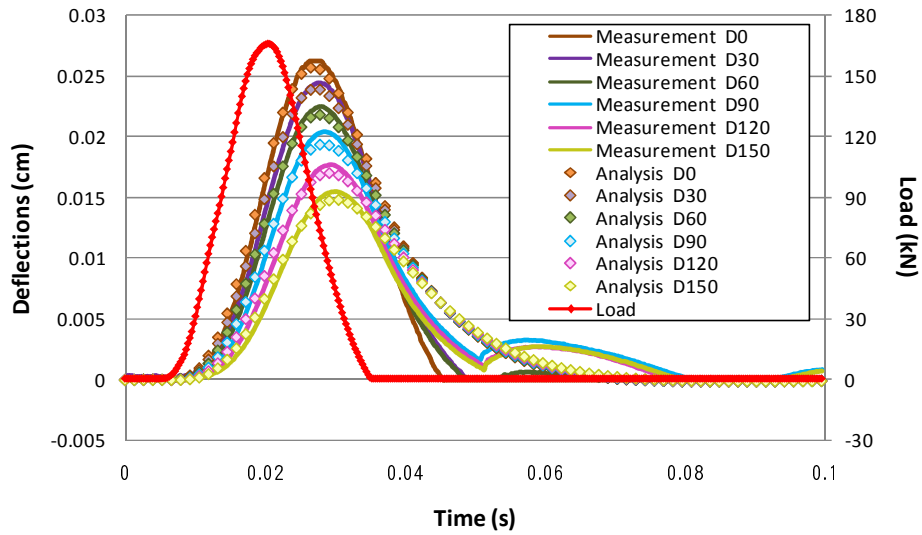


Figure 5(a) Comparison of Measured and Computed Deflections (Section 1)

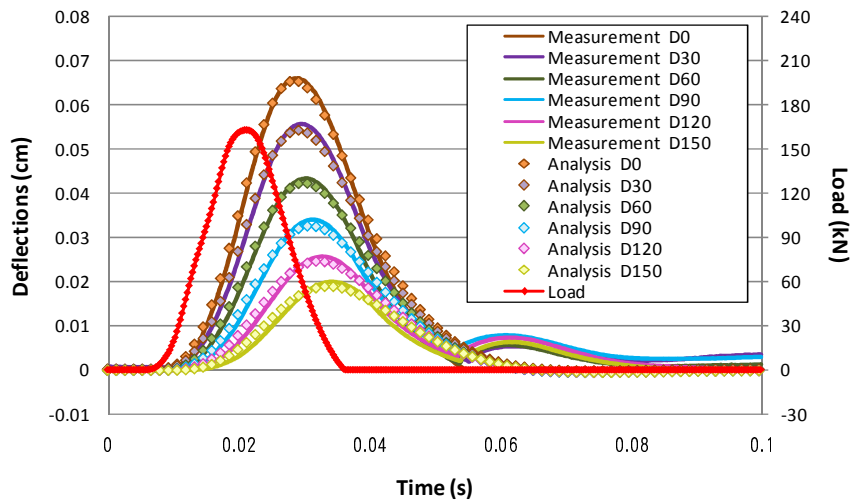


Figure 5(b) Comparison of Measured and Computed Deflections (Section 2 Loading Area)

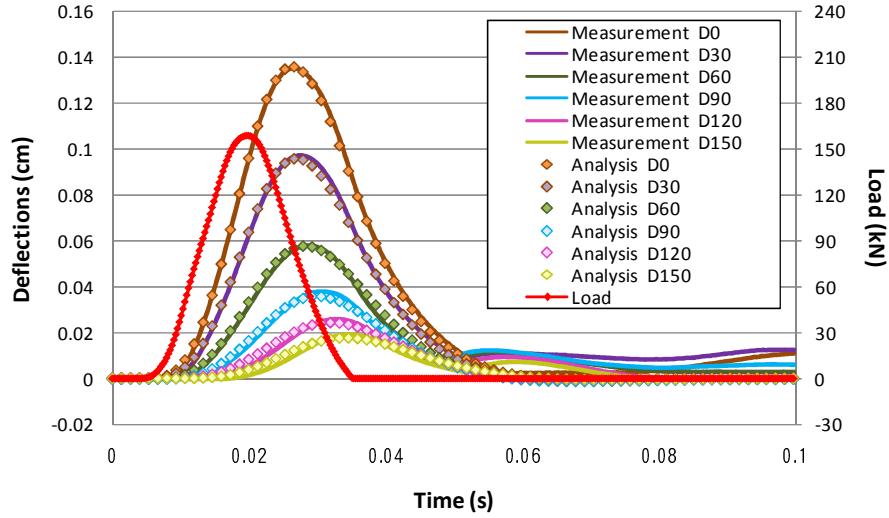


Figure 5(c) Comparison of Measured and Computed Deflections (Section 3 Loading Area)

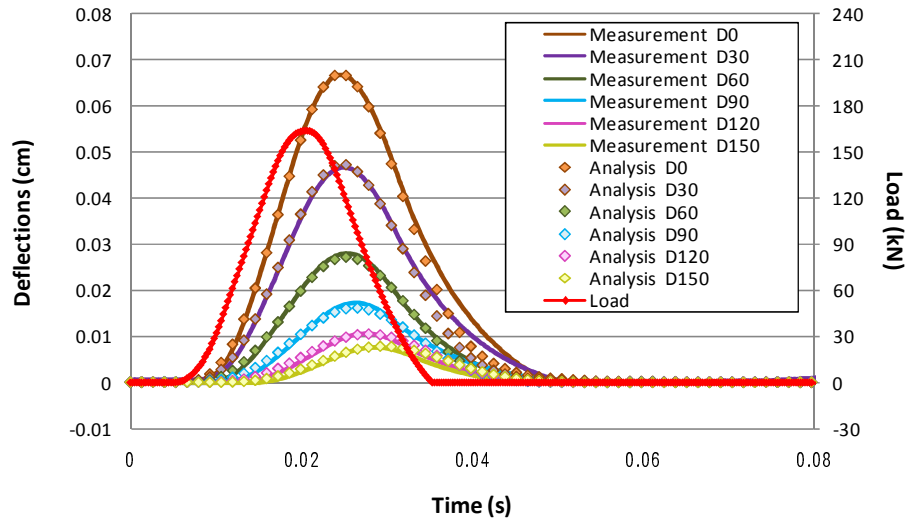


Figure 5(d) Comparison of Measured and Computed Deflections (Section 4 Loading Area)

## COMPUTED STRAINS

Strains of section 2 are computed using both three and four layer systems. Figure 6(a) shows a horizontal strain  $\epsilon_x$  at the bottom of asphalt stabilized layer in Section 2 in both no loading area and loading area. The significant increase in the strain is observed in loading area compared with that of no loading area. The difference in strains of no loading area and loading area is much greater in four layer system than in three layer system. Figure 6(b) compares the vertical strains at the top of subgrade of Section 2. The difference in strains at no loading area and loading area is negligibly small. However there is clear difference in strains between the four layer system and the three layer system. This may be due to the difference in mechanical

properties between layer 1 (asphalt) and layer 2 (asphalt stabilized) although they are classified as P401. Considering the maximum subgrade strains are in the order of  $1/1,000$ , a linear elastic model can be used for the analysis [9].

The advantage of analytical solution used here is that it can compute responses at any point of interest in a pavement structure.

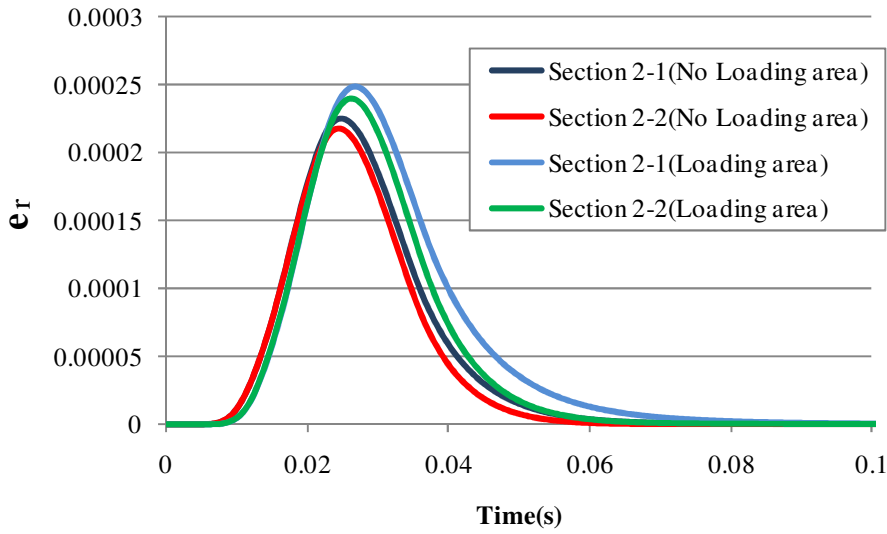


Figure 6(a) Computed Horizontal Strains at the Bottom of Asphalt Stabilized Layer (Section 2)

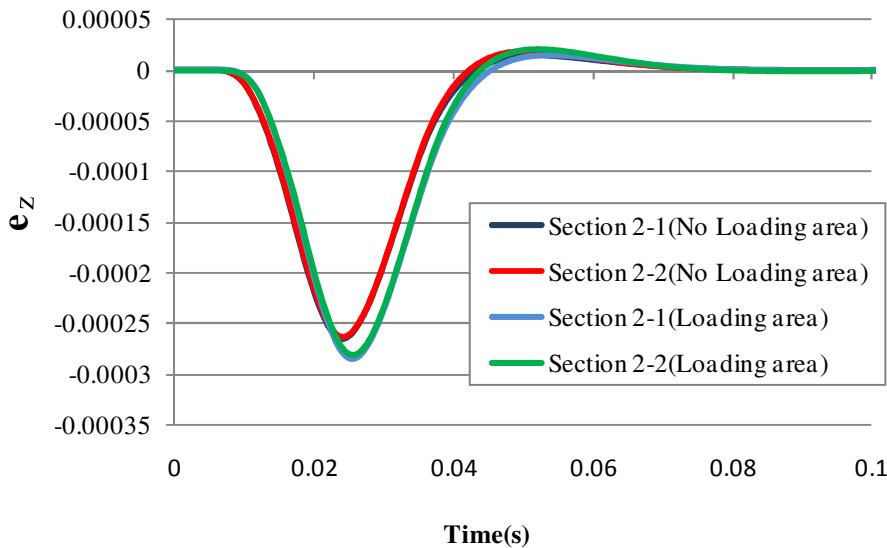


Figure 6(b) Computed Vertical Strains at the top of Sub-grade (Section 2)

## SUMMARY AND CONCLUSIONS

Backcalculation was performed using FWD time history data measured at the Federal Aviation Administration's National Airport Test Facility. The backcalculation software used here is called Wave\_BALM recently developed by authors, in which the analytical solutions of wave propagation equations (WPALS) are implemented.

Test pavement sections are modeled by three or four layer systems assuming subgrade thickness is infinite. After backcalculation, measured and computed deflections are compared and found excellent agreement. From backcalculated results in Table 3, the following comments can be made,

- 1) Estimated PCC modulus is about 24,500 MPa which is a little too large and estimated econocrete modulus is about 13,000 MPa. It seems the identified results appears to be little small. This may be due to the assumption that layer inter face is fully bonded.
- 2) In section 2, the estimated modulus of asphalt stabilized layer is found about 5,000 MPa, while the modulus of asphalt layer 8,400 MPa. However the both layers are classified as P401, the estimated modulus of combined layer is 6,800 MPa.
- 3) Layer moduli of no loading area and those of loading area significantly differ at the subgrade of low strength.
- 4) Table 4 presents layer damping coefficients. They are found less than 1% of layer moduli. However, it is not known how closely they are related to pavement condition.
- 5) Responses such as displacements, strains and stresses can be computed at any point of interest.

Effected most in backcalculation is the range of seed values. They must be assigned with great care. The next is layer thickness. If layer thickness error is 15% or more, the iterative steps used in this backcalculation may not converge. The effect of layer density has not been fully examined yet. Its error effect seems greater than the effect of Poisson's ratio.

## ACKNOWLEDGEMENTS

The writers thank the Federal Aviation Association for kindly providing us the FWD test data, which made possible to conduct this work. Acknowledgement is also given to Dr. Edward Guo for his advice and comments. This work was supported by Grant-in-Aid for Scientific Research (C) (20560435) in Japan.

## REFERENCES

1. Uzan, J., Dynamic Linear Backcalculation of Pavement Material Parameters, *Journal of Transportation Engineering*, ASCE, Vol. 120, No. 1, 109-126, 1994.
2. Matsui, K., Dong, Q., Hachiya, Y. and Takahashi, O., Difference in estimated layer moduli from static and dynamic backcalculations. *Proceedings of the 2002 FAA Airport Technology Transfer Conference*, Atlantic City, New Jersey, USA, May 5 – 8, 2002.
3. Matsui, K., Maina, J. W., Dong, Q., and Sasaki, Y., A fast dynamic backcalculation of layer moduli using axi-symmetric approach. *International Journal of Pavements (IJP)*, Volume 2, Number 1-2. 75-87. USA 2003.
4. Chatti K., Ji, Y.G., Harichandran, R.S., Dynamic Time Domain Backcalculation of Layer Complex Moduli and Thicknesses in Asphalt Concrete Pavements, CD-ROM, Transportation Research Board, National Research Council, Washington, D.C., 2004.
5. Matsui, K., Hachiya, Y., Maina, W.J., Kikuta, Y. and Nagae, T., Influence of Seed Layer Moduli on Finite Element Method-Based Modulus Backcalculation Results, *Transportation Research Record* 1951, TRB, National Research Council, Washington, D.C. 122-136, 2006.
6. Ozawa, Y. and Matsui, K., Wave Propagation Analysis of Pavement Structures Composed of Voigt Model, *Journal of JSCE, Division E*, Vol.64, No.2, 314-322, 2008.4. (in Japanese)
7. Takehara, K., Ozawa, Y., Omoto, S. and Matsui, K., Mechanistic Model of Pavement Structure Considering Wave Form of FWD Surface Deflections, *Journal of Pavement Engineering*, JSCE, Vol.14, 139-146, 2009.12. (in Japanese)
8. Ozawa, Y., Shinohara, Y. Matsui, K. and Higashi, S., Structural Evaluation of Multi-layered Viscoelastic Media Using Wave Propagation Theory, *Journal of JSCE, Division E*, Vol.64, No.4, 533-540, 2008.10. (in Japanese)
9. Goto, S., Burland, J.B. and Tatsuoka, F., Nonlinear Soil Model With Various Strain Levels and Its Application to Axisymmetric Excavation Problem, *Soils and Foundations*, Vol.39, No.4, 111-119, 1999.